The Molecular Genetics and Evolution of Red and Green Color Vision in Vertebrates

Shozo Yokoyama and F. Bernhard Radlwimmer

Department of Biology, Syracuse University, Syracuse, New York 13244

Manuscript received March 19, 2001
Accepted for publication May 29, 2001

ABSTRACT

To better understand the evolution of red-green color vision in vertebrates, we inferred the amino acid sequences of the ancestral pigments of 11 selected visual pigments: the LWS pigments of cave fish (*Astyanax fasciatus*), frog (*Xenopus laevis*), chicken (*Gallus gallus*), chameleon (*Anolis carolinensis*), goat (*Capra hircus*), and human (*Homo sapiens*); and the MWS pigments of cave fish, gecko (*Gekko gekko*), mouse (*Mus musculus*), squirrel (*Sciurus carolinensis*), and human. We constructed these ancestral pigments by introducing the necessary mutations into contemporary pigments and evaluated their absorption spectra using an *in vitro* assay. The results show that the common ancestor of vertebrates and most other ancestors had LWS pigments. Multiple regression analyses of ancestral and contemporary MWS and LWS pigments show that single mutations S180A, H197Y, Y277F, T285A, A308S, and double mutations S180A/H197Y shift the λ_{max} of the pigments by −7, −28, −8, −15, −27, and 11 nm, respectively. It is most likely that this "five-sites" rule is the molecular basis of spectral tuning in the MWS and LWS pigments during vertebrate evolution.

HUMAN color vision is achieved through three types of photosensitive molecules: short wavelength- (or blue-) sensitive (SWS), middle wavelength- (or green-) sensitive (MWS), and long wavelength- (or red-) sensitive (LWS) visual pigments, which absorb light maximally (λ_{max}) at ~420, ~530, and ~560 nm, respectively (Boynton 1979). However, having only SWS pigments and either MWS or LWS pigments, most mammals have dichromatic color vision. This condition is commonly known as "red-green color blindness." Even in human, the "red-green color blindness" is relatively common, affecting ~8% of males (Kalmus 1965). When diverse species are surveyed, the λ_{max} of most LWS pigments ranges from 550 to 560 nm, while the MWS pigments detect a wider range of light with λ_{max} at ~510–540 nm (Yokoyama 2000a). All of these pigments belong to a specific evolutionary group, often referred to as the LWS/MWS group (Yokoyama and Yokoyama 1996; Yokoyama 1997, 1999, 2000a; Ebrey and Koutalos 2001).

Each visual pigment consists of a chromophore, 11-*cis*-retinal, and a transmembrane protein, opsin, which is encoded by a specific opsin gene. The SWS, MWS, and LWS opsin genes were cloned for the first time from human (Nathans *et al.* 1986). Since then, the mechanisms of spectral tuning in the MWS and LWS pigments of vertebrates have been studied extensively. It was shown that the spectral sensitivities of the MWS and LWS pigments in human and fish are determined mainly by A180/F277/A285 (amino acids A, F, and A at sites 180, 277, and 285, following the amino acid site numbers in the human LWS/MWS pigments, respectively) and S180/Y277/T285, respectively (Yokoyama and Yokoyama 1990; Neitz *et al.* 1991; Chan *et al.* 1992; Merbs and Nathans 1993; Asenjo *et al.* 1994). The spectral sensitivities of some MWS pigments from such species as mouse (*Mus musculus*), rat (*Rattus norvegicus*), and rabbit (*Oryctolagus cuniculus*), however, cannot be explained by this "three-sites" rule and require amino acid changes at two entirely new sites: 197 and 308 (Sun *et al.* 1997; Radlwimmer and Yokoyama 1998; Yokoyama and Radlwimmer 1998, 1999). It was suggested that S180A (amino acid replacement S → A at site 180), H197Y, Y277F, T285A, and A308S shift the λ_{max} of the LWS/MWS pigments toward green by 7, 28, 7, 15, and 16 nm, respectively, and the reverse changes toward red by the same amounts (Yokoyama and Radlwimmer 1999). This five-sites rule explains the λ_{max} of virtually all LWS/MWS pigments of vertebrates. The MWS pigment of bottlenose dolphin (*Tursiops truncatus*) is an exception, where the observed λ_{max} is 13 nm lower than the expected value from this five-sites rule (Yokoyama and Radlwimmer 1999). Thus, the details of the mechanisms of spectral tuning in the MWS and LWS pigments are still not fully understood.

The evolution of red-green color vision was also studied by inferring the amino acid sequences at the five critical sites of the ancestral pigments. Comparing the MWS and LWS pigments from human and fish (*Astyanax fasciatus*), it was suggested that the LWS pigments in these species evolved from the ancestral MWS pigment independently (Yokoyama and Yokoyama 1990). The

Corresponding author: Shozo Yokoyama, Biological Research Laboratories, Department of Biology, Syracuse University, 130 College Pl., Syracuse, NY 13244. E-mail: syokoyam@mailbox. syr.edu

evolution of the LWS pigment from the MWS pigment was also suggested by Jacobs (1993) and Winderickx *et al.* (1992), but the primate ancestor appears to have had the LWS pigment (Nei *et al.* 1997). It is also speculated that the mammalian ancestor had the MWS pigment (Yokoyama and Radlwimmer 1999). In these analyses, the absorption spectra of ancestral pigments were not evaluated. Without having the actual absorption spectra of the ancestral pigments, the evolutionary results of red-green color vision remain speculative. However, once the amino acid sequences and λ_{max} of such ancestral visual pigments are determined, we can study not only the evolutionary processes of LWS/MWS pigments directly but also the molecular bases of red-green color vision through time.

Here, we infer the amino acid sequences of ancestral pigments from contemporary sequences, construct the ancestral pigments, evaluate their λ_{max}, and test the validity of the five-sites rule during vertebrate evolution. To accomplish the first three goals, we consider 11 pigments: the LWS pigments of human, goat (*Capra hircus*), American chameleon (*Anolis carolinensis*), chicken (*Gallus gallus*), clawed frog (*Xenopus laevis*), and cave fish (*A. fasciatus*) and the MWS pigments of human, squirrel (*Sciurus carolinensis*), mouse (*M. musculus*), gecko (*Gekko gekko*), and cave fish (*A. fasciatus*). The results suggest that virtually all ancestral pigments had amino acids SHYTA (amino acids S, H, Y, T, and A at sites 180, 197, 277, 285, and 308, respectively) and were red sensitive. Statistical and mutagenesis analyses show that the five-sites rule, now including the synergistic effect of amino acid sites 180 and 197, fully explains the variation in the spectral sensitivity of all ancestral and currently known LWS/MWS pigments in vertebrates, including the dolphin MWS pigment.

MATERIALS AND METHODS

cDNA cloning and DNA sequencing: Total retinal RNAs of chicken (*Gallus gallus*) and frog (*Xenopus laevis*) are gifts from Dr. Mary Pierce at the SUNY Upstate Medical University at Syracuse, and that of cave fish (*A. fasciatus*) was isolated using the procedure of Yokoyama *et al.* (1995). Figure 1 shows reverse transcription (RT)-PCR primers used to amplify the four types of full-length opsin cDNAs.

For each set of primers, cDNA was reverse transcribed at 42° for 1 hr and at 95° for 5 min, and then PCR was carried out for 30 cycles at 94° for 45 sec, 55° for 1.5 min, and 72° for 2 min. PCR products were gel isolated and subcloned into the T-tailed *Eco*RV-digested Bluescript plasmid vector with T-overhang attached to 3′ ends (Hadjeb and Berkowitz 1996). Nucleotide sequences of the entire region of the cDNA clones were determined by cycle sequencing reactions using the Sequitherm Excell II long-read kits (Epicentre Technologies, Madison, WI) with dye-labeled M13 forward and reverse primers. Reactions were run on a LI-COR (Lincoln, NE) 4200LD automated DNA sequencer.

Expression and spectral analyses of pigments: The PCR-amplified opsin cDNAs were subcloned into the *Eco*RI and *Sal*I restriction sites of the expression vector pMT5 (Khorana *et al.* 1988). These plasmids were expressed in COS1 cells by transient transfection. The pigments were regenerated by incubating the opsins with 11-*cis*-retinal (Storm Eye Institute, Medical University of South Carolina) and purified using immobilized 1D4 (The Culture Center, Minneapolis, MN) in buffer W1 [50 mm *N*-(2-hydroxyethyl) piperazine-*N*′-2-ethanesulfonic acid (HEPES; pH 6.6), 140 mm NaCl, 3 mm $MgCl_2$, 20% (w/v) glycerol, and 0.1% dodecyl maltoside], as previously described (Yokoyama 2000b).

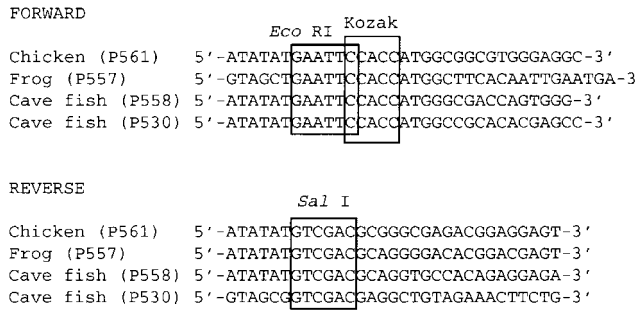

Figure 1.—Oligonucleotide primers for RT-PCR amplification of red and green opsin mRNAs. The *Eco*RI and *Sal*I sites are boxed in the forward and reverse primers, respectively, and were used for cloning into the expression vector pMT5. A Kozak sequence (CCACC) was inserted between the *Eco*RI site and the initiation codon to promote translation.

Mutants were generated by using the QuickChange site-directed mutagenesis kit (Stratagene, La Jolla, CA). All DNA fragments that were subjected to mutagenesis were sequenced to rule out spurious mutations. UV-visible spectra were recorded at 20° using a Hitachi U-3000 dual beam spectrophotometer. Visual pigments were bleached for 3 min using a 60-W standard light bulb equipped with a Kodak Wratten #3 filter at a distance of 20 cm. Data were analyzed using Sigmaplot software (Jandel Scientific, San Rafael, CA).

Sequence data analyses: The sources of the amino acid sequences of the MWS and LWS pigments of different vertebrate species are given in Table 1, where both of their amino acid sequences and λ_{max} are known. So far, with the exception of the chicken, frog, and cave fish pigments, their λ_{max}'s have been evaluated using *in vitro* assay.

We selected two fish, two frog, two reptile, and one bird LWS/MWS pigments (Table 1). The numbers of mammalian pigments with λ_{max} at ~510, ~530, and ~560 nm are 4, 7, and 6, respectively (Table 1), from which we selected 1, 2, and 2 pigments, respectively. Thus, with respect to the phylogenetic and spectral diversities, these 11 pigments represent every segment of currently known LWS/MWS pigments in vertebrates. The phylogenetic relationship of fish, frog, reptiles, and mammals is well established (*e.g.*, see Kumar and Hedges 1998), but that of human, goat, and rodents is unclear (Novacek 1992; De Jong 1998; Shoshani and McKenna 1998; Huchon *et al.* 1999; Liu and Miyamoto 1999; Waddell *et al.* 1999a,b; Madsen *et al.* 2001; Murphy *et al.* 2001). Thus, they are assumed to be equally distantly related. Accordingly, we consider the phylogenetic relationship [((((human (P560), human (P530)), goat (P553), (squirrel (P532), mouse (P508))), ((chameleon (P560), gecko (P527)), chicken (P561))), frog (P557)), (cave fish (P558), cave fish (P530))]. On the basis of this tree topology, we infer the ancestral sequences of the opsins by using a computer program, PAML, based on a likelihood-based Bayesian method (Yang *et al.* 1995; Yang 1997). In the inference, paralogous bovine RH1 (GenBank accession no. U49742), goldfish RH2 (L11865),

TABLE 1

Vertebrate LWS and MWS pigments

Pigment	Accession no.	Absorption spectrum	
		λ_{max} (nm)	Reference
Human (P560)[a]	M13300	560[b]	Oprian *et al.* (1991)
Human (P552)	M13300[c]	552 ± 1	Merbs and Nathans (1992)
Human (P530)[a]	K03490	530[b]	Oprian *et al.* (1991)
Marmoset (P561)	AF051582	561 ± 1	Yokoyama and Radlwimmer (1999)
Marmoset (P553)	AF051588	553 ± 1	Yokoyama and Radlwimmer (1999)
Marmoset (P539)	AF051594	539 ± 1	Yokoyama and Radlwimmer (1999)
Goat (P553)[a]	U67999	553 ± 1	Radlwimmer and Yokoyama (1997)
Deer (P531)	AF132041	531 ± 1	Yokoyama and Radlwimmer (1999)
Dolphin (P524)	AF055457	524[b]	Fasick *et al.* (1998)
Horse (P545)	AF132043	545 ± 1	Yokoyama and Radlwimmer (1999)
Cat (P553)	AF132040	553 ± 1	Yokoyama and Radlwimmer (1999)
Rabbit (P509)	AF054235	509 ± 1	Radlwimmer and Yokoyama (1998)
Guinea pig (P516)	AF132042	516 ± 1	Yokoyama and Radlwimmer (1999)
Squirrel (P532)[a]	AF132044	532 ± 1	Yokoyama and Radlwimmer (1999)
Mole rat (P534)	AF139726	534 ± 4	David-Gray *et al.* (1999)
Mouse (P508)[a]	AF011389	508 ± 2	Sun *et al.* (1997)
Rat (P509)	AF054246	509 ± 1	Radlwimmer and Yokoyama (1998)
Chicken (P561)[a]	M62903	561 ± 1	This study
Pigeon (P559)	AF149248	559 ± 2	Kawamura *et al.* (1999)
Zebra finch (P560)	AF222333	560 ± 3	Yokoyama *et al.* (2000)
Chameleon (P560)[a]	U08131	560 ± 1	Kawamura and Yokoyama (1998)
Gecko (P527)[a]	M92036	527 ± 3	N. S. Blow (unpublished data)
Frog (P557)[a]	U90895	557 ± 5	This study
Goldfish (P559)	L11867	559 ± 4	Yokoyama and Radlwimmer (1999)
Cave fish (P558)[a]	M90075	558 ± 2	This study
Cave fish (P530)[a]	M38619	530 ± 2	This study

Cat, *Felis catus*; cave fish, *Astyanax fasciatus*; chameleon, *Anolis carolinensis*; chicken, *Gallus gallus*; deer, *Odocoileus virginianus*; dolphin, *Tursiops truncatus*; frog, *Xenopus laevis*; gecko, *Gekko gekko*; goat, *Capra hircus*; goldfish, *Carassius auratus*; guinea pig, *Cavia porcellus*; horse, *Equus caballus*; human, *Homo sapiens*; marmoset, *Callithrix jacchus*; mole rat, *Spalax ehrenbergi*; mouse, *Mus musculus*; pigeon, *Columba livia*; rabbit, *Oryctolagus cuniculus*; rat, *Rattus norvegicus*; squirrel, *Sciurus carolinensis*; zebra finch, *Taeniopygia guttata*.

[a] Sequences used to infer the ancestral pigments of vertebrates.

[b] No standard error is provided.

[c] See also Winderickx *et al.* (1992).

chameleon SWS1 (AF134194), and chicken SWS2 (M92037) pigments were used as the outgroup (for the description of these classes of pigments, see Yokoyama and Yokoyama 1996; Yokoyama 1997, 1999, 2000a; Ebrey and Koutalos 2001).

To study the spectral sensitivities of ancestral mammalian pigments further, we consider yet another phylogenetic tree of LWS/MWS pigments: [(((human (P560), human (P530)), (marmoset (P562), marmoset (P553), marmoset (P540))), rabbit (P509), (goat (P553), deer (P531))), guinea pig (P516), (squirrel (P532), mouse (P508))]. This tree topology of the mammalian pigments is basically the same as that in Yokoyama and Radlwimmer (1999). However, it contains three trifercations because of unresolved phylogenetic relationships among the mammalian species.

RESULTS

Absorption spectra of the chicken, frog, and cave fish LWS/MWS pigments: To study the mechanisms of spectral tuning of visual pigments, we applied the *in vitro* assay (Yokoyama 2000a) to the LWS/MWS pigments of chicken, frog, and cave fish. The regenerated pigments show two absorption peaks, one at ~280 nm and another at 530–561 nm (Figure 2). When these pigments are exposed to light, the second peak shifts to ~380 nm (results not shown), indicating the *cis-trans* isomerization of the chromophore (Hubbard and Kropf 1958). This control experiment demonstrates that the lower peaks are entirely due to opsins covalently linked to 11-*cis*-retinal via a Schiff base bond. When measured in the dark, the LWS pigments of cave fish, frog, and chicken have λ_{max} at 558 ± 2, 557 ± 2, and 561 ± 2 nm, respectively, while the MWS pigment of cave fish has a λ_{max} at 530 ± 2 nm (Figure 2, Table 1). The respective dark-light difference spectra are given by 557, 557, 561, and 531 nm, all of which are also precise to within ±2 nm (Figure 2, insets) and are very close to the corresponding dark spectra.

Previously, using a 3-[(3-cholamidopropyl) dimethylammonio]-1-propanesulfonate-phosphatidylcholine

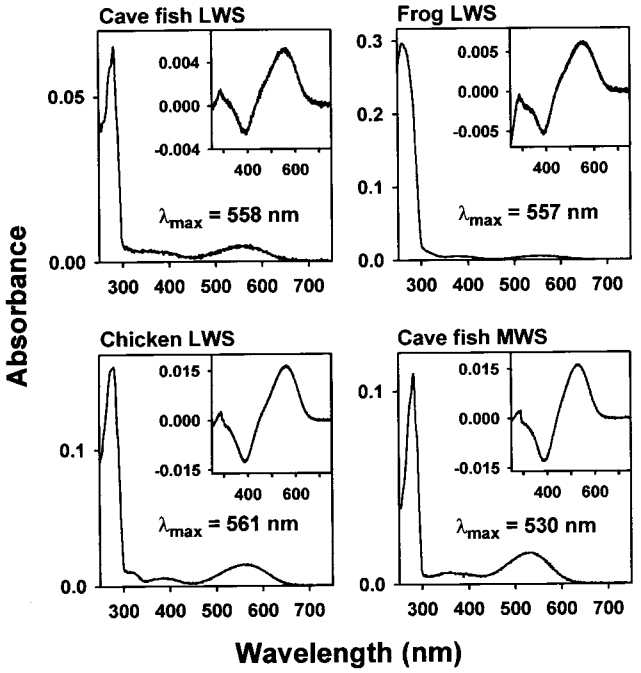

FIGURE 2.—Absorption spectra of the cave fish LWS, frog LWS, chicken LWS, and cave fish MWS pigments measured in the dark. The dark-light difference spectra are shown in the insets.

(CHAPS-PC) mixture and microspectrophotometry (MSP) methods, the λ_{max} of the chicken LWS pigment were estimated to be 571 (OKANO *et al.* 1989) and 569 nm (BOWMAKER and KNOWLES 1977), respectively. Our estimate is ~10 nm lower than these values. The cause of this difference is not immediately clear. However, in the CHAPS-PC method, the sample used for the evaluation of the λ_{max} is not pure and contains ~92% of the LWS pigments, while the MSP analyses are often subject to sampling errors. Compared with these methods, the visual pigments regenerated using an *in vitro* assay are identical and are expected to provide a more reliable λ_{max} of each specific pigment.

The two previous estimates of the λ_{max} of frog (P557) pigment are very different: 611 nm by MSP (WITKOVSKY *et al.* 1981) and 533 nm by the light-evoked cone contraction method (BESHARSE and WITKOVSKY 1992). At present, the cause of the two very different estimates is not clear. Our estimate of 557 nm falls in between these two λ_{max}'s. MSP estimates for the cave fish MWS and LWS pigments regenerated with 11-*cis*-retinal showed λ_{max}'s at 533 ± 3 and 563 ± 4 nm, respectively (F. I. HAROSI and J. KLEINSCHMIDT, personal communication; see also KLEINSCHMIDT and HAROSI 1992). The present results, 530 and 558 nm, respectively, agree well with the MSP results. In the following, we use the dark spectra obtained from the *in vitro* assay for the λ_{max} of the chicken, frog, and cave fish pigments (Table 1).

Amino acid sequences of the ancestral LWS/MWS pigments: Given the tree topology of the vertebrate pigments in Figure 3, the amino acid sequences of the ancestral pigments at nodes a–i (pigments *a–i*, respectively) were inferred by using the JTT model of amino acid replacements (JONES *et al.* 1992; Figure 4). As we can see in Figure 4, the accuracy of most inferred amino acids is quite high and only relatively small numbers of them have posterior probabilities of <0.9. Note that the inferred amino acid sequences of pigments *g* and *h* are identical. When the Dayhoff model of amino acid replacements (DAYHOFF *et al.* 1978) is used, very similar ancestral amino acid sequences are inferred. For pigments *a–f*, *g* (= *h*), and *i*, the two models predict only three, one, five, one, zero, one, three, and two amino acid differences, respectively. At these ambiguous sites, the posterior probabilities associated with the amino acid inference are always <0.9.

Using the contemporary pigments, we suggested that the spectral sensitivities of the LWS/MWS pigments are controlled mainly by the amino acids at 180, 197, 277, 285, and 308 (YOKOYAMA and RADLWIMMER 1998, 1999). At these five critical sites, pigments *a–e*, *g* (= *h*), and *i* have SHYTA, while pigment *f* has SYYTA (Figure 3). Most of these inferred amino acids have posterior probabilities >0.9. For pigments *d–f*, however, amino acids S180 and A180 are predicted with probabilities of 0.7 and 0.3, respectively.

Absorption spectra of the ancestral pigments: Many inferred amino acids of the ancestral pigments are identical to those of the contemporary pigments (Figure 4), showing that pigments *a–i* can be constructed by introducing necessary mutations into some extant pigments. Indeed, pigments *d–f* were constructed by introducing six mutations into human (P560) pigment, nine mutations into pigment *d*, and nine mutations into squirrel (P532) pigment, respectively (Figure 5A). The amino acid sequences of pigments *a–c*, *g* (= *h*), and *i* are similar to that of chameleon (P560) pigment, which can be divided into segments I–IV by three restriction sites (Figures 4 and 5B). Thus, by introducing necessary mutations into these segments, we constructed I1–I4, II1–II4, III1–III4, and IV1–IV2, respectively (Figure 5C). The pigments *a–c*, *g* (= *h*), and *i* were then obtained by recombining these four segments at the three restriction sites (Figure 5C). In this way, we constructed one ancestral pigment at each node, each amino acid having the highest posterior probability.

When measured in the dark, the λ_{max} of pigments *a–f*, *g* (= *h*), and *i* are 563 ± 2, 563 ± 2, 561 ± 2, 558 ± 2, 558 ± 2, 536 ± 1, 561 ± 2, and 564 ± 2 nm, respectively (Figure 6). The respective dark-light difference spectra are given by 564, 563, 561, 558, 558, 536, 561, and 564 nm, all of which are precise to within ±2 nm (Figure 6, insets). They are virtually identical to the corresponding dark spectra. Thus, pigment *f* with SYYTA at the five critical sites has a λ_{max} at 536 nm, while the other ancestral pigments with SHYTA have λ_{max} at 558–564 nm (Figures 3 and 6). These results suggest that the pigment of the common ancestor was red sensitive and the con-

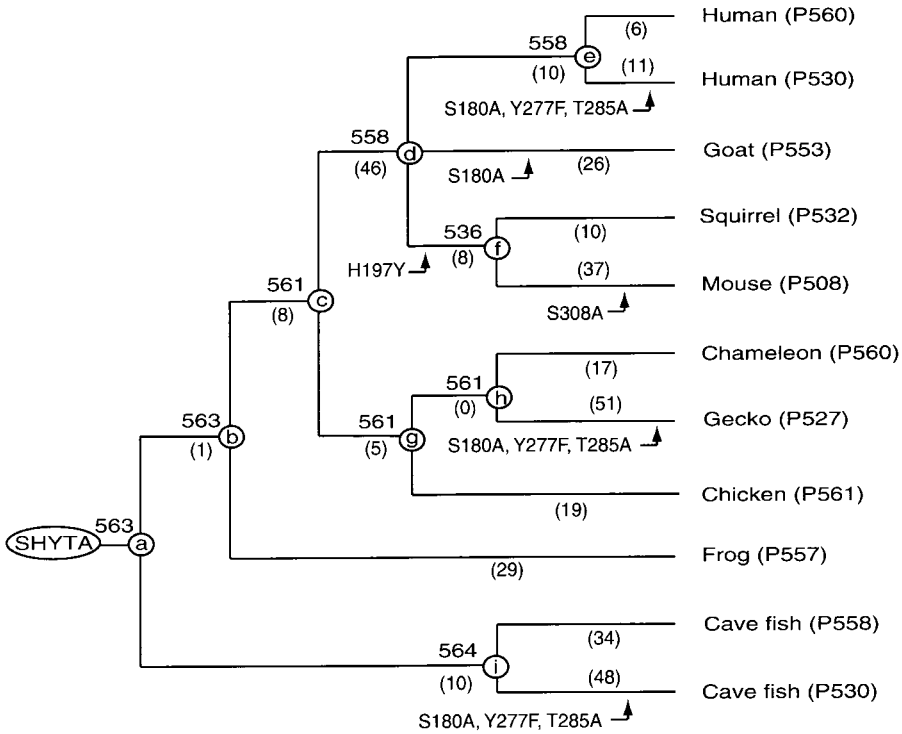

FIGURE 3.—A composite evolutionary tree topology of 11 vertebrate LWS/MWS pigments. SHYTA refers to the amino acids at sites 180, 197, 277, 285, and 308 for the ancestral vertebrate pigment. The numbers after P and those at the nodes a–i refer to λ_{max} obtained by *in vitro* assay. The numbers in parentheses indicate the total numbers of amino acid replacements along a specific branch.

temporary LWS/MWS pigments evolved from the LWS pigment. As noted earlier, for pigments *d–f*, S180 and A180 are predicted with probabilities 0.7 and 0.3, respectively. As we see below, changes S180A and A180S should shift the λ_{max} for no more than 7 nm and, therefore, the uncertain inference of amino acids at site 180 does not change the red and green sensitivities of the ancestral pigments.

Now, what do the spectral sensitivity data in Figure 3 tell us about the mechanisms of spectral tuning in the LWS and MWS pigments? Following YOKOYAMA and RADLWIMMER (1999), let θ_{180}, θ_{197}, θ_{277}, θ_{285}, θ_{308}, and Z be the magnitudes of the λ_{max} shifts caused by S180A, H197Y, Y277F, T285A, A308S, and the absorption spectrum of a pigment with SHYTA. Note that the amino acid compositions for all contemporary and ancestral pigments are either Y277/T285 (Y277 and T285) or F277/A285 (Figure 4) and, therefore, two parameters, θ_{277} and θ_{285}, cannot be estimated separately. When multiple linear regression analysis is applied to the λ_{max} of the 11 contemporary and 9 ancestral pigments, $\hat{\theta}_{180} = -7 \pm 2$ nm, $\hat{\theta}_{197} = -26 \pm 2$ nm, $\hat{\theta}_{277}/\hat{\theta}_{285} = -24 \pm 3$ nm, $\hat{\theta}_{308} = -19 \pm 4$ nm, and $Z = 560 \pm 1$ nm. When the regression analysis is applied to only the 11 contemporary pigments, $\hat{\theta}_{180} = -6 \pm 2$ nm, $\hat{\theta}_{197} = -27 \pm 2$ nm, $\hat{\theta}_{277}/\hat{\theta}_{285} = -24 \pm 2$ nm, $\hat{\theta}_{308} = -18 \pm 3$ nm, and $Z = 559 \pm 1$ nm. Thus, the two sets of estimates are practically identical. Using the former set of estimates, we can predict the expected λ_{max} for the contemporary and ancestral pigments (Table 2). Table 2 shows that the observed λ_{max} of frog (P557) and cave fish (P558) pigments and ancestral pigments *a*, *b*, *d*, *e*, and *i* fall outside of the 95% confidence interval. However, considering the standard errors associated with the estimation of the λ_{max}, the expected and corresponding observed λ_{max}'s are in reasonably good agreement.

Table 2 clearly shows that the spectral tuning of the LWS/MWS pigments is determined mainly by the amino acids at 180, 197, 277, 285, and 308. It is also true that, despite having the same amino acid composition SHYTA at the five critical sites, pigments *a–e*, *g* (= *h*), and *i* have somewhat different λ_{max}, ranging from 558 to 564 nm (Figures 3 and 6). Among these, the λ_{max} of pigments *d* and *e* (both with $\lambda_{max} = 558$ nm) and that of pigment *i* ($\lambda_{max} = 564$ nm) are significantly different ($P < 0.05$). Where does this variation in the λ_{max} values come from? As noted earlier, the spectral sensitivities of human (P530) and human (P560) pigments are determined mainly by the three-sites rule. However, additional amino acid differences at sites 116, 230, 233, and 309 are known to have some minor influence on the differentiation of the two pigments (ASENJO *et al.* 1994). Pigments *d*, *e*, and *i* have two identical amino acids I230/Y309, but pigments *d* and *e* have two amino acid replacements S116Y/A233S (Figure 4). Both amino acids Y116 and S233 are human (P530) pigment specific. Therefore, the difference in the λ_{max} between pigments *d* and *e* and pigment *i* is caused most probably by the slightly decreased λ_{max} in the former two pigments due to S116Y/A233S. It should be stressed, however, that the minor variation in λ_{max} is found only in certain mammalian pigments. Thus, this minor adjustment in the mechanisms of spectral tuning seems to be a local phenomenon.

Five-sites rule: Using the contemporary and ancestral pigments in Figure 3, we could not infer θ_{277} and θ_{285}

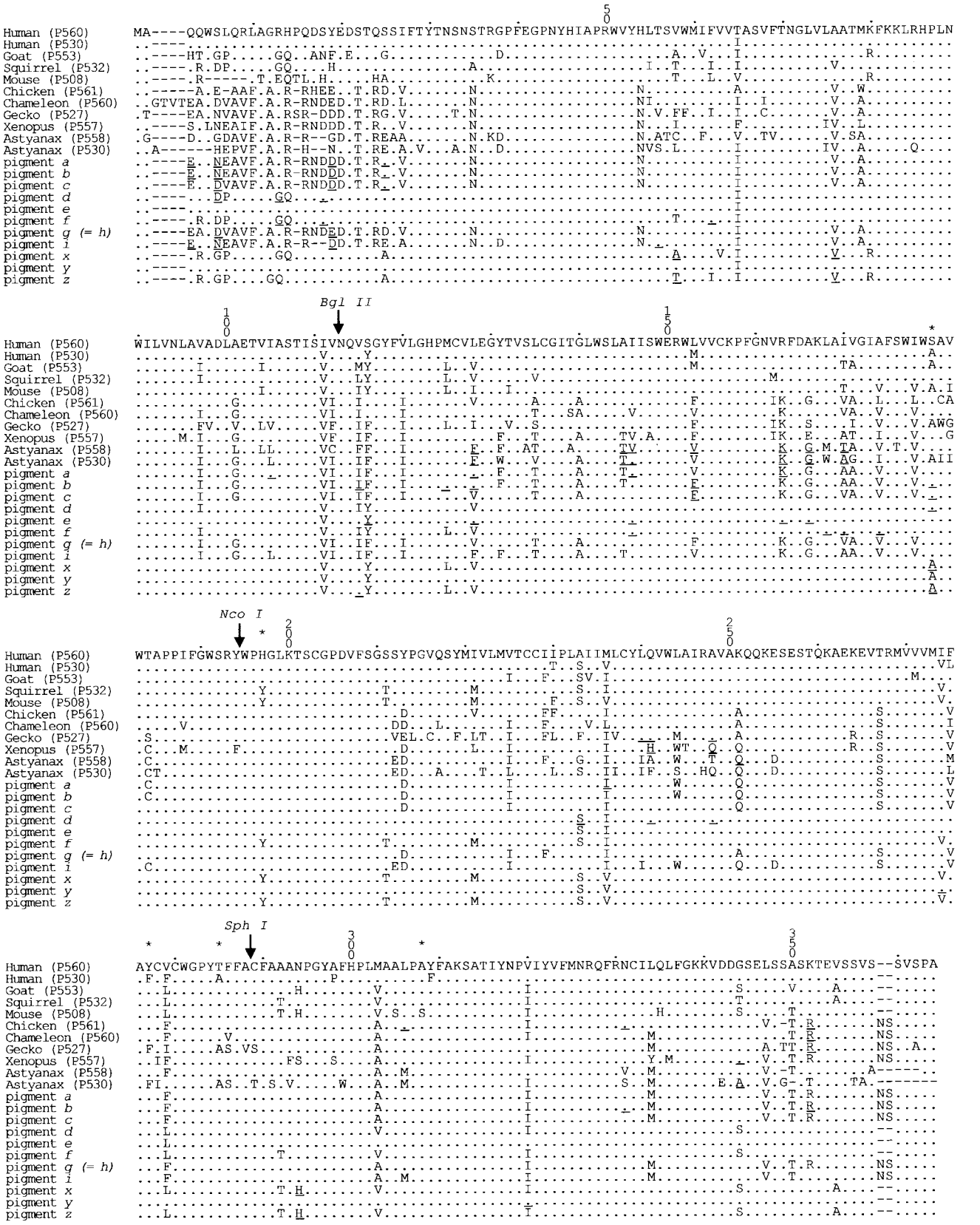

FIGURE 4.—Aligned amino acid sequences of the red and green pigments in vertebrates. The numbers after P refer to λ_{max} obtained by *in vitro* assays. Dots indicate the identity of the amino acids with those of the human (P560) pigment. The positions of five critical sites, 180, 197, 277, 285, and 308, are marked by asterisks. The ancestral amino acids that have a probability of 90% or less are underlined. *Bgl*II, *Nco*I, and *Sph*I denote the positions of three restriction sites.

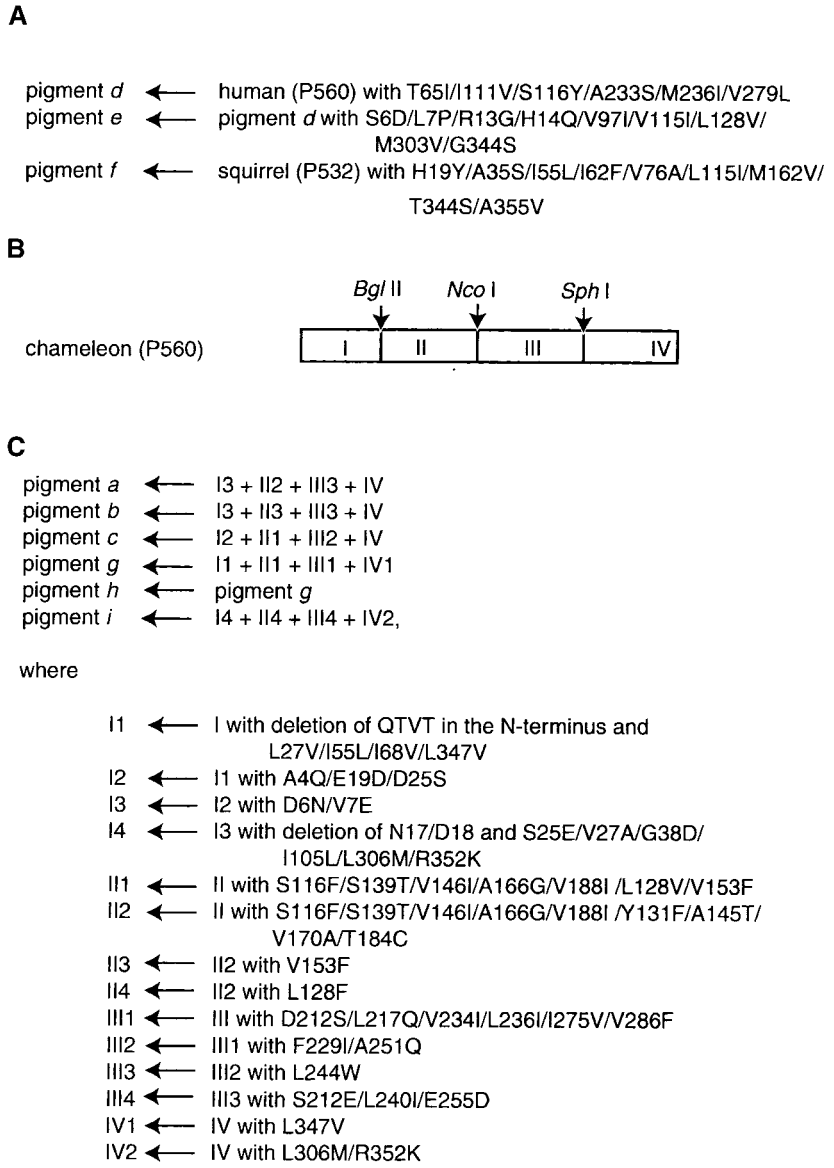

FIGURE 5.—Strategy for constructing the ancestral pigments *a-i*. (A) The construction of pigments *d–f* from human (P560) and squirrel (P532) pigments. (B) The opsin cDNA structure of chameleon (P560) pigment. *Bgl*II, *Nco*I, and *Sph*I denote the positions of three restriction sites (see also Figure 4). (C) The construction of pigments *a–c*, *g* (= *h*), and *i* from chameleon (P560) pigment.

separately. However, if we consider the amino acid sequences of all 26 pigments in Table 1, we can evaluate θ_{277} and θ_{285} separately and also determine interactions between sites 180 and 197 ($\theta_{180\times197}$); 180 and 285 ($\theta_{180\times285}$); 197 and 285 ($\theta_{197\times285}$); 197 and 308 ($\theta_{197\times308}$); 277 and 285 ($\theta_{277\times285}$); and 180, 277, and 285 ($\theta_{180\times277\times285}$; APPENDIX).

When the interaction terms are neglected, $Z = 559$ nm, $\hat{\theta}_{180} = -5$ nm, $\hat{\theta}_{197} = -22$ nm, $\hat{\theta}_{277} = -8$ nm, $\hat{\theta}_{285} = -17$ nm, and $\hat{\theta}_{308} = -25$ nm (Table 3, model a). When the λ_{max} for the 26 pigments are estimated by using these θ values, they agree reasonably well with the corresponding observed values (Table 4, column a). However, the λ_{max} of dolphin (P524) and squirrel (P532) pigments deviate from the corresponding expected values by 5 and 4 nm, respectively (see also YOKOYAMA and RADLWIMMER 1999). The 95% confidence intervals for the λ_{max} values of dolphin (P524) and squirrel (P532) pigments are 526–532 nm and 533–539 nm, respectively. The corresponding observed λ_{max} fall outside of these intervals. Thus, some improvement in the estimation procedure is desirable. It turns out that such an improvement can be made by considering interactions among the five critical sites. The improvement in the estimation procedures with and without a specific interaction term can be tested by

$$F_{20,19} = (\mathrm{SSE}_2/20)/(\mathrm{SSE}_1/19),$$

where SSE_1 and SSE_2 indicate the SSE values (see APPENDIX) for the models with and without a specific interaction term, respectively. When interaction terms $\theta_{180\times197}$, $\theta_{180\times285}$, $\theta_{197\times285}$, $\theta_{197\times308}$, $\theta_{277\times285}$, and $\theta_{180\times277\times285}$ are considered separately, the $F_{20,19}$ values are 3.4 ($P < 0.001$), 1.2 ($P = 0.25$–0.5), 1.2 ($P = 0.25$–0.5), 1.6 ($P = 0.1$–0.25), 1.0 ($P \cong 0.5$), and 1.0 ($P \cong 0.5$), respectively. These tests show that only the estimation procedure with $\theta_{180\times197}$ should significantly improve the estimates.

If we include an interaction term $\theta_{180\times197}$, then $Z =$

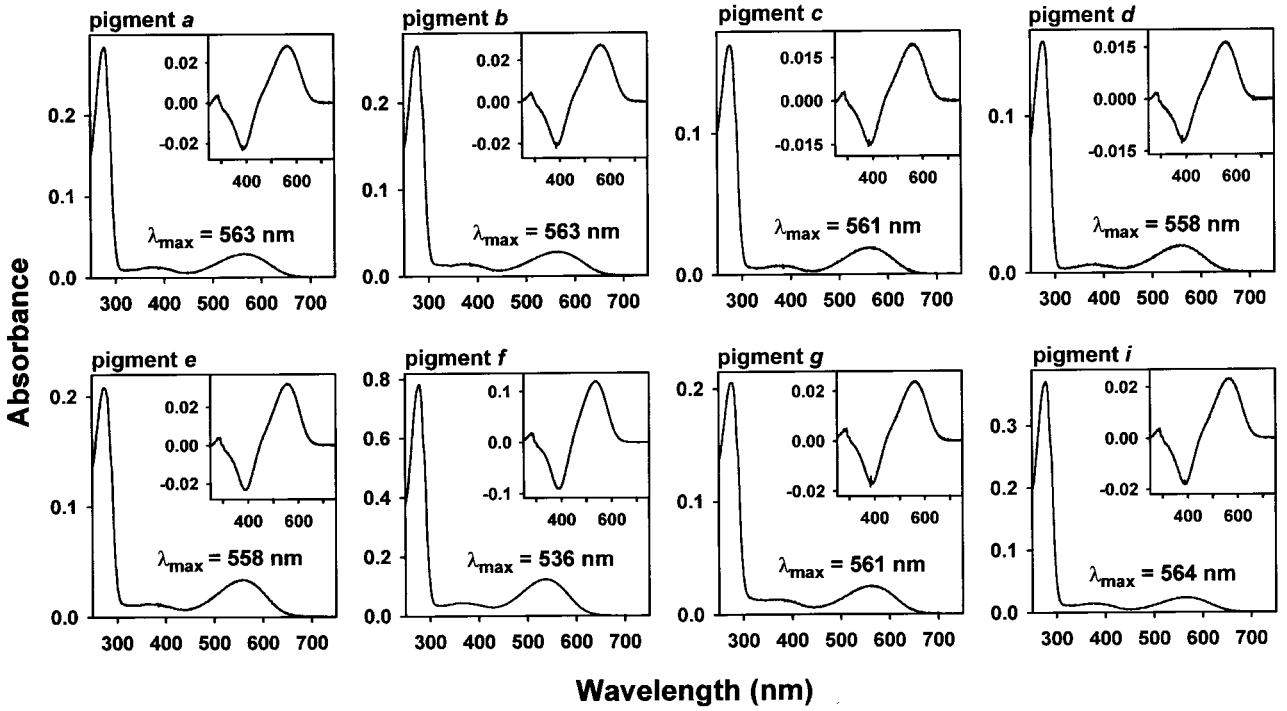

FIGURE 6.—Absorption spectra of the ancestral pigments *a–g* and *i* measured in the dark. The dark-light difference spectra are shown in the insets.

559 nm, $\hat{\theta}_{180} = -7$ nm, $\hat{\theta}_{197} = -28$ nm, $\hat{\theta}_{277} = -8$ nm, $\hat{\theta}_{285} = -15$ nm, $\hat{\theta}_{308} = -27$ nm, and $\hat{\theta}_{180\times197} = 11$ nm (Table 3, model b). Thus, *Z*, $\hat{\theta}_{180}$, $\hat{\theta}_{277}$, $\hat{\theta}_{285}$, and $\hat{\theta}_{308}$ are similar to those of model a, but $\hat{\theta}_{197}$ decreases and, at the same time, $\hat{\theta}_{180\times197}$ causes a significant red shift in the λ_{max}. When the expected λ_{max} of the 26 pigments are inferred using these estimates, the differences between the expected and observed λ_{max} are significantly reduced (Table 4, column b). The 95% confidence intervals for the λ_{max} of dolphin (P524) and squirrel (P532) pigments are now 523–528 nm and 529–534 nm, respectively, and contain the observed λ_{max}.

TABLE 2

The λ_{max} of LWS/MWS pigments

Pigment	λ_{max} (nm)	
	Observed	Expected[b]
Human (P560)	560[a]	560 (559–562)
Human (P530)	530[a]	529 (526–532)
Goat (P553)	553 ± 1	553 (548–558)
Squirrel (P532)	532 ± 1	534 (531–537)
Mouse (P508)	508 ± 1	508 (503–513)
Chicken (P561)	561 ± 2	560 (559–562)
Chameleon (P560)	560 ± 3	560 (559–562)
Gecko (P527)	527 ± 5	529 (526–532)
Frog (P557)	557 ± 2	560 (559–562)
Cave fish (P558)	558 ± 2	560 (559–562)
Cave fish (P530)	530 ± 2	529 (526–532)
Pigment *a*	563 ± 2	560 (559–562)
Pigment *b*	563 ± 2	560 (559–562)
Pigment *c*	561 ± 2	560 (559–562)
Pigment *d*	558 ± 2	560 (559–562)
Pigment *e*	558 ± 2	560 (559–562)
Pigment *f*	536 ± 1	534 (531–537)
Pigment *g* (= *h*)	561 ± 2	560 (559–562)
Pigment *i*	564 ± 2	560 (559–562)

[a] No standard error is given.
[b] Values in parentheses show 95% confidence intervals.

These analyses show that the five-sites rule, now including the synergistic effect of sites 180 and 197, explains the λ_{max} of all contemporary pigments. According to the five-sites rule, the ancestral pigments with SHYTA and SYYTA should have λ_{max} at 559 and 536 nm, respectively. The corresponding observed values are 558–564 and 536 nm (Figure 3). Thus, this rule explains the spectral tunings of the LWS/MWS pigments during the entire history of vertebrate evolution. Sites 180, 277, 285, and 308 are located near the chromophore (PALCZEWSKI *et al.* 2000), where interaction between the chromophore and an opsin usually takes place (YOKOYAMA 2000a,b; EBREY and KOUTALOS 2001). The site 197 is located outside of the transmembrane regions, but H197 is known for its important function of chloride binding (SUN *et al.* 1997). Although we cannot offer a structural explanation for the λ_{max} shift, it suggests an intimate relationship between the chloride binding site at 197 and the spectral tuning residue at 180.

Ancestral mammalian pigments: By applying the JTT model of amino acid replacements to another tree topology of the mammalian pigments (Figure 7), we also

TABLE 3

The effects of amino acid changes at sites 180, 197, 277, 285, and 308 on the λ_{max} shifts

	Estimator (nm)						
Model	Z	$\hat{\theta}_{180}$	$\hat{\theta}_{197}$	$\hat{\theta}_{277}$	$\hat{\theta}_{285}$	$\hat{\theta}_{308}$	$\hat{\theta}_{180\times197}$
a. No interaction	559 ± 1	−5 ± 1	−22 ± 1	−8 ± 2	−17 ± 2	−25 ± 2	—
b. One interaction	559 ± 1	−7 ± 1	−28 ± 1	−8 ± 1	−15 ± 1	−27 ± 1	11 ± 2

inferred the amino acid sequences of the common ancestors of the 11 mammalian pigments (pigment *x*), of human (P560) and human (P530) pigments (pigment *y*), and of squirrel (P532) and mouse (P508) pigments (pigment *z*). Pigments *x*–*z* roughly correspond to pigments *d*–*f* in Figure 3, respectively. Most amino acids inferred have posterior probabilities of >0.9 and pigments *x*–*z* have only four, two, and five sites, where the posterior probabilities are <0.9 (Figure 4).

Using site-directed mutagenesis and recombinant DNA techniques, we then reconstructed these three ancestral pigments. Again, using an *in vitro* assay, the λ_{max} of pigments *x*–*z* are determined to be 533 ± 1, 553 ± 1, and 533 ± 2 nm, respectively (Figures 7 and 8). These results are consistent with those of Yokoyama and Radlwimmer (1999). However, we have also seen that the λ_{max} of pigments *d*–*f* are given by 558, 558, and 536 nm, respectively (see Figure 3). Thus, the λ_{max} of pigment *x* is 25 nm lower than that of pigment *d*.

Pigments *x*–*z* have AYYTA, AHYTA, and AYYTA at the five critical sites, respectively, whereas pigments *d*–*f* have SHYTA, SHYTA, and SYYTA, respectively. Thus, the difference between the λ_{max} of pigments *x* and *d* must have been caused by the amino acid differences at sites 180 and 197. Slightly lower λ_{max} of pigments *y* and *z* than those of pigments *e* and *f* can be explained

TABLE 4

Amino acid compositions at five critical sites and λ_{max} of the extant LWS and MWS pigments

	Sites					λ_{max} (nm) expected (expected − observed)[a]	
Pigment	180	197	277	285	308	a	b
Human (P560)	S	H	Y	T	A	559 (−1)	559 (−1)
Human (P552)	A	H	Y	T	A	554 (−2)	553 (1)
Human (P530)	A	H	F	A	A	529 (−1)	530 (0)
Marmoset (P561)	S	H	Y	T	A	559 (−2)	559 (−2)
Marmoset (P553)	A	H	Y	T	A	554 (1)	553 (0)
Marmoset (P539)	A	H	Y	A	A	537 (−2)	538 (−1)
Goat (P553)	A	H	Y	T	A	554 (1)	553 (0)
Deer (P531)	A	H	F	A	A	529 (−2)	530 (−1)
Dolphin (P524)	A	H	Y	T	S	529 (5)	526 (2)
Horse (P545)	A	H	F	T	A	546 (1)	545 (0)
Cat (P553)	A	H	Y	T	A	554 (1)	553 (0)
Rabbit (P509)	A	Y	Y	T	S	507 (−2)	508 (−1)
Guinea pig (P516)	S	Y	Y	A	A	519 (3)	517 (1)
Squirrel (P532)	S	Y	Y	T	A	536 (4)	531 (−1)
Mole rat (P534)	A	Y	Y	T	A	532 (−2)	536 (2)
Rat (P509)	A	Y	Y	T	S	507 (−2)	508 (1)
Mouse (P508)	A	Y	Y	T	S	507 (1)	508 (0)
Chicken (P561)	S	H	Y	T	A	559 (−2)	559 (−2)
Pigeon (P559)	S	H	Y	T	A	559 (0)	559 (0)
Zebra finch (P560)	S	H	Y	T	A	559 (−1)	559 (−1)
Chameleon (P560)	S	H	Y	T	A	559 (−1)	559 (−1)
Gecko (P527)	A	H	F	A	A	529 (2)	530 (3)
Frog (P557)	S	H	Y	T	A	559 (2)	559 (2)
Goldfish (P559)	S	H	Y	T	A	559 (0)	559 (0)
Cave fish (P558)	S	H	Y	T	A	559 (1)	559 (1)
Cave fish (P530)	A	H	F	A	A	529 (−1)	530 (0)

[a] a and b denote estimation procedures with no interaction and with an interaction between 180 and 197, respectively.

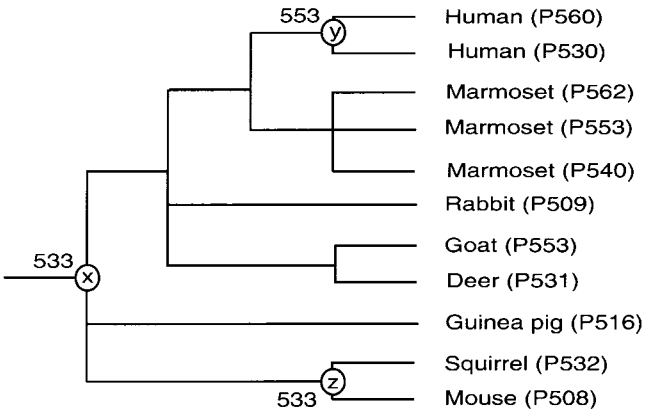

FIGURE 7.—A composite evolutionary tree topology of 11 mammalian LWS/MWS pigments. The numbers after P and those at the nodes x–z refer to λ_{max} obtained by *in vitro* assay.

by the amino acid differences at site 180. These results clearly show that the inference of the ancestral pigments depends not only on the phylogenetic relationship of extant pigments but also on the types of pigments used for constructing the phylogenetic tree. As noted earlier, however, the phylogenetic relationship of mammalian species has not been resolved. Thus, until the issue is resolved, it is premature to discuss whether the mammalian ancestor had MWS or LWS pigment.

Compared with the variability in the spectral sensitivities of those of the mammalian pigments, the λ_{max} of LWS/MWS pigments of nonmammalian vertebrates are more uniform. The currently available data show that all fish, amphibian, reptile, and avian lineages have LWS pigments but not necessarily MWS pigments (Table 1). Similarly, the orthologous pigment in marine lamprey (*Lamptera marinus*) has P180, Y277, and T285, showing the LWS pigment-specific feature (H. Zhang and S. Yokoyama, unpublished data). It seems that the divergence between chameleon (P560) and gecko (P527) pigments (Figure 3, node h) and between cave fish (P558) and cave fish (P530) pigments (node i) occurred ~150–190 million years (MY) ago (Yokoyama and Blow 2001) and ~190–320 MY ago (Yokoyama and Yokoyama 1990), respectively. The divergence between the two human pigments is estimated to be ~30 MY ago (Yokoyama and Yokoyama 1989). Thus, the divergences of the LWS and MWS pigments seem to be relatively recent events in vertebrate evolution. These observations are consistent with our suggestion that the vertebrate ancestor had the LWS pigment rather than the MWS pigment.

TABLE 5

Effects of single amino acid changes on the λ_{max} shift

Pigment	Mutation	λ_{max} (nm)
Pigment *x*	—	532
	A180S	533
	A58T, V76A, H294N	532
Pigment *y*	—	553
	I274V	554
	I320V	553
Pigment *z*	—	532
	T58A	532
	V115I, A180S	534
	H294N	533
	V76A	532

DISCUSSION

It is highly likely that the vertebrate ancestor possessed the LWS pigment with SHYTA at the five critical amino acid sites and that the contemporary LWS/MWS pigments evolved from the ancestral LWS pigment. We have also seen that the five-sites rule, now including the synergistic effect between amino acid sites 180 and 197, fully explains the variation in the λ_{max} of the LWS/MWS pigments during the entire history of vertebrate evolution. The first conclusion was based on a single amino acid sequence at each ancestral node, while the second conclusion was derived using a purely statistical argument. Here, we address these points in more detail.

Uncertain inference of amino acids and spectral sensitivity: As noted earlier, ancestral mammalian pigments *x*–*z* have 4, 2, and 5 amino acid sites where the posterior probabilities are <0.9. We replaced these amino acids by those with the second highest posterior probabilities

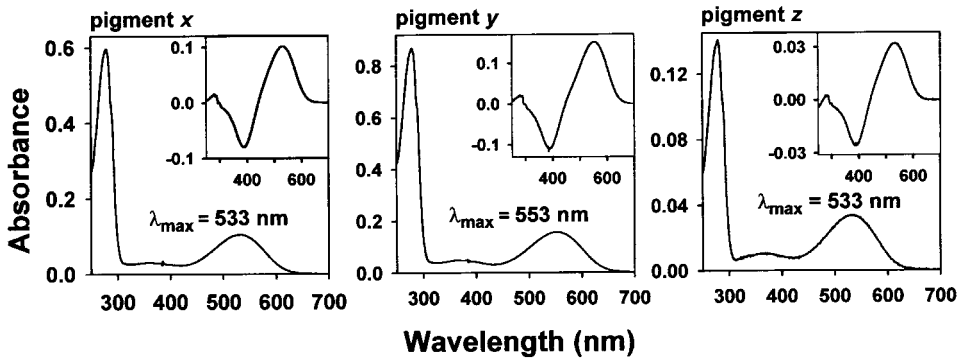

FIGURE 8.—Absorption spectra of the ancestral pigments *x*–*z* measured in the dark. The dark-light difference spectra are shown in the insets.

TABLE 6

Amino acid changes at the five critical sites of pigment *x* and their λ_{max}

Mutation[a]	λ_{max} (nm)	Contemporary pigment
AYYTA[b]	533 ± 1	Mole rat (P534)
AHYTA	553 ± 1	Human (P552), marmoset (P553), goat (P553), cat (P553)
SHYTA	557 ± 2	Human (P560), marmoset (P561), chicken (P561), pigeon (P559), zebra finch (P560), chameleon (P560), frog (P557), cave fish (P558), goldfish (P559)
AHFAA	530 ± 2	Human (P530), deer (P531), gecko (P527), cave fish (P530)
AHYAA	537 ± 2	Marmoset (P539)
AYYTS	509 ± 1	Mouse (P508), rat (P509), rabbit (P509)
AYYAA	519 ± 1	Guinea pig (P516)
SYYTA	532 ± 1	Squirrel (P532)
AHYTS	523 ± 2	Dolphin (P524)
AHFTA	545 ± 1	Horse (P545)

[a] Each mutation is indicated by an underline.
[b] Amino acid composition of pigment *x*.

and determined the λ_{max} of the mutant pigments. The results clearly show that the λ_{max} of the regenerated mutant pigments are virtually identical to those without such mutations, showing that the amino acid differences at these 11 sites have little effect on the λ_{max} shift (Table 5).

Interestingly, amino acid changes A180S introduced into pigments *x* and *z* do not shift the λ_{max} either. Considering $\hat{\theta}_{180}$ of −7 nm (Table 3, model b), this observation may be surprising. These results need to be understood, however, by considering the interaction between sites 180 and 197. Note that squirrel (P532) and mole rat (P534) pigments have AYYTA and SYYTA at the five critical sites, respectively, but their λ_{max} values are 532 and 534 nm and are virtually identical (Table 4). On the other hand, human (P552), marmoset (P553), goat (P553), and cat (P553) pigments have AHYTA, whereas human (P560), marmoset (P561), chicken (P561), pigeon (P560), zebra finch (P560), chameleon (P560), frog (P557), cave fish (P558), and goldfish (P559) pigments all have SHYTA (Table 4). The λ_{max} of the two groups of pigments differ by 4–9 nm (Table 4). Thus, the λ_{max} shift caused by A108S is very small, if there is any, for pigments with Y197, but it is ~7 nm for pigments with H197. From these observations, it is expected that since both pigments *x* and *z* have AYYTA, A180S should not cause any significant λ_{max} shift.

More on the five-sites rule: The statistical inferences strongly suggest that the five-sites rule explains the variation in the λ_{max} of all contemporary and ancestral LWS/MWS pigments. When the five critical sites are considered, the contemporary LWS/MWS pigments are classified into nine different groups (Table 6). To test the validity of the statistical result further, we reconstructed the nine types of pigments by modifying the amino acid compositions at the five critical sites of pigment *x*. Using the *in vitro* assay, the λ_{max} of these mutant pigments are measured. Table 6 clearly shows that, as long as the amino acid compositions at the five critical sites are the same, the λ_{max} of the mutants are virtually identical to those of the corresponding contemporary pigments.

It should be stressed that these mutant pigments with the background of pigment *x* and the corresponding contemporary LWS/MWS pigments can have very different amino acid compositions at sites other than the 5 critical sites. For example, reflecting dynamic evolutionary processes of amino acid replacements during vertebrate evolution, pigment *x* differs from human (P560) pigment at 27 amino acid sites, whereas it differs from cave fish (P558) pigment at 91 sites. Thus, the majority of these amino acid replacements have contributed very little to the spectral tuning in the LWS/MWS pigments and may be considered as "neutral" changes. The mutagenesis analyses using the mammalian ancestral pigment strengthen the argument that the "five-sites" rule has been the molecular mechanism of spectral tuning in the LWS/MWS pigments throughout vertebrate evolution.

Red-green color vision: To study the structure-function relationships of the LWS/MWS pigments, we considered only the visual pigments with 11-*cis*-retinal (also known as vitamin A_1 aldehyde). In nature, however, the λ_{max} of these visual pigments can be modified further at the visual pigment level as well as at the photoreceptor cell level. It turns out that many fishes, amphibians, and reptiles can use 11-*cis*-3, 4-dehydroretinal (or vitamin A_2 aldehyde) as the chromophore, which causes a red shift in the λ_{max} (Whitmore and Bowmaker 1989; Harosi 1994). For example, goldfish (P559) pigment uses mostly vitamin A_2 aldehyde as the chromophore and actually achieves a λ_{max} value at ~620 nm (Palacios *et al.* 1998; Yokoyama and Radlwimmer 1999). Cave fish (P558) pigment uses vitamin A_1 and A_2 aldehydes with equal frequencies as the chromophore (Kleinschmidt

and Harosi 1992). Thus, this pigment can achieve a λ_{max} at ~560–620 nm depending upon the composition of the chromophore. Cone photoreceptor cells in many amphibians, reptiles, and birds use different devices, colored oil droplets. Although their exact functions have not been fully elucidated, the oil droplets often contain a high concentration of carotenoids and are likely to serve as cutoff filters (Bowmaker 1991). Both chicken (P561) and pigeon (P559) pigments are expressed in the cone cells with the red-colored oil droplets with cutoff wavelengths at 560–580 nm (Bowmaker *et al.* 1997). These photoreceptor cells may actually achieve λ_{max} at 600–620 nm (Bowmaker and Knowles 1977). Thus, the photoreceptor cells with the LWS pigments in many vertebrate species actually detect more reddish light than the LWS pigments regenerated using the *in vitro* assay. By the same token, when vitamin A_2 aldehyde is used as the chromophore, the MWS pigments can also achieve λ_{max} at ~560 nm (see Palacios *et al.* 1998).

When the actual λ_{max} of visual pigments are red shifted, how do animals achieve λ_{max} at ~530 nm? It turns out that many species use an evolutionarily distantly related group of RH2 pigments for their green color detection (Yokoyama 2000a,b; Ebrey and Koutalos 2001). For example, by replacing vitamin A_1 aldehyde with vitamin A_2 aldehyde, the two goldfish RH2 pigments shift their λ_{max} from ~510 nm to 530–540 nm (Johnson *et al.* 1993; Palacios *et al.* 1998). The chicken photoreceptor cell with the RH2 pigments with λ_{max} at ~510 nm actually achieves a λ_{max} at 533 nm due to the presence of a green oil droplet in the cell (Bowmaker and Knowles 1977). Like the MWS pigments, these RH2 pigments are often called "green pigments," sometimes creating confusing terminology. Placental mammals use neither vitamin A_2 aldehyde nor colored oil droplets and, therefore, their red-green color vision is determined directly by the MWS and LWS pigments.

Vitamin A_1 aldehyde is used by both vertebrates and invertebrates, but a vitamin A_2 aldehyde-based pigment has not been found in invertebrates (Smith and Goldsmith 1990). Thus, vitamin A_2 aldehyde might have been an evolutionary device to generate dual functions or a new function of one visual pigment. Similarly, as suggested by Thompson (1991), colored oil droplets might have been an efficient way to generate a variability in the spectral sensitivity in photoreceptors that had not yet achieved the mechanisms for expressing a single type of visual pigment in one photoreceptor cell (however, see Walls 1942). While these functional changes are underway in the RH2 pigments, it is reasonable to assume that the ancestor of the LWS/MWS pigments or photoreceptor cells with such pigments must have been red sensitive. These observations are also consistent with the idea that the vertebrate ancestor had the LWS pigment.

Purifying selection and adaptive evolution: For visual pigments, the numbers of amino acid replacements (K) can differ considerably between comparable branches. In Figure 3, for example, compared with the K for branch b-frog (P557) pigment (29), those for b-gecko (P527), b-mouse (P508), b-squirrel (P532), b-goat (P553), b-human (P530), and b-human (P560) pigments are 64, 99, 72, 80, 75, and 70, respectively. These values are all $\geqslant 29$ ($P < 0.01$). This difference is largely due to the accelerated evolution in the mammalian ancestor, represented by branch c–d. Similarly, the K for branches f-mouse (P508) pigment and h-gecko (P527) pigment are significantly larger than those for f-squirrel (P532) pigment and h-chameleon (P560) pigment, respectively (both with $P < 0.01$; Figure 3).

These results seem to show that the accelerated evolutionary rate of amino acid replacement leads to the acquisition of new functions. More specifically, the K tend to be larger for branches where amino acid replacements occur at the functionally important five sites 180, 197, 277, 285, and 308 than those without such changes. Furthermore, the gecko pigment has pure rod-retinas (Crescitelli 1972; Crescitelli *et al.* 1977) and the cone-specific MWS pigment had to adapt to this unique cellular change. The accelerated evolutionary rate of amino acid replacement for branch c–d is not immediately clear, but it may reflect the λ_{max} shift from 558 nm to either 536 nm in the ancestral rodent pigment or 553 nm of the goat pigment (Figure 3). If it turns out that the rodents are most distantly related to the other groups of mammals, then the K associated with H197Y in the ancestral rodent pigment will be >8. On the other hand, if the goat pigment is most distantly related, then the K associated with S180A can be >26. Thus, there is a positive correlation between the evolutionary rate of amino acid replacement and the level of the divergence in the λ_{max}. Such correlation has also been detected for various evolutionary groups of visual pigments in the gecko (Yokoyama and Blow 2001) and avian species (Yokoyama *et al.* 2000). All of these examples seem to show that the relaxation from purifying selection caused by environmental changes is the first important step toward the adaptation of organisms to new environments.

Comments by Ruth Yokoyama, Stephen Schaeffer, and two anonymous reviewers are greatly appreciated. This work was supported by National Institutes of Health grant GM-42379.

LITERATURE CITED

Asenjo, A. B., J. Rim and D. D. Oprian, 1994 Molecular determinants of human red/green color discrimination. Neuron **12:** 1131–1138.

Besharse, J. C., and P. Witkovsky, 1992 Light-evoked contraction of red absorbing cones in the *Xenopus* retina is maximally sensitive to green light. Vis. Neurosci. **8:** 243–249.

Bowmaker, J. K., 1991 The evolution of vertebrate visual pigments and photoreceptors, pp. 63–81 in *Evolution of the Eye and Visual Systems*, edited by J. R. Cronly-Dillon and R. L. Gregory. CRC Press, Boca Raton, FL.

Bowmaker, J. K., and A. Knowles, 1977 The visual pigments and oil droplets of the chicken retina. Vision Res. **17:** 755–764.

Bowmaker, J. K., L. A. Heath, S. E. Wilkie and D. M. Hunt, 1997 Visual pigments and oil droplets from six classes of photoreceptor in the retinas of birds. Vision Res. **37:** 2183–3194.

Boynton, R. M., 1979 *Human Color Vision*. Holt, Rinehart & Winston, New York.

Chan, T., M. Lee and T. P. Sakmar, 1992 Introduction of hydroxyl bearing amino acids causes bathochromic spectral shifts in rhodopsin: amino acid substitutions responsible for red-green color pigment spectral tuning. J. Biol. Chem. **267:** 9478–9480.

Crescitelli, F., 1972 The visual cells and visual pigments of the vertebrate eye, pp. 245–363 in *Handbook of Sensory Physiology*, edited by H. J. A. Dartnall. Springer, Berlin.

Crescitelli, F., H. J. A. Dartnall and E. R. Loew, 1977 The visual pigments of gecko and other vertebrate eye, pp. 391–450 in *Handbook of Sensory Physiology*, edited by H. J. A. Dartnall. Springer, Berlin.

David-Gray, Z. K., H. M. Cooper, J. W. Janssen, E. Nevo and R. G. Foster, 1999 Spectral tuning of a circadian photopigment in a subterranean 'blind' mammal (*Spalax ehrenbergi*). FEBS Lett. **461:** 343–347.

Dayhoff, M. O., R. M. Schwartz and B. C. Orcutt, 1978 A model of evolutionary change in proteins, pp. 345–352 in *Atlas of Protein Sequence and Structure*, Vol. 5, Suppl. 3, edited by M. O. Dayhoff. National Biomedical Research Foundation, Washington, DC.

De Jong, W. W., 1998 Molecules remodel the mammalian tree. Trends Ecol. Evol. **13:** 270–275.

Ebrey, T., and Y. Koutalos, 2001 Vertebrate photoreceptors. Prog. Retin. Eye Res. **20:** 49–94.

Fasick, J. I., T. W. Cronin and D. M. Hunt, 1998 The visual pigments of the bottlenose dolphin (*Tursiops truncatus*). Vis. Neurosci. **15:** 643–651.

Hadjeb, N., and G. A. Berkowitz, 1996 Preparation of T-overhang vectors with high PCR product cloning efficiency. Biotechniques **20:** 20–22.

Harosi, F. I., 1994 Analysis of two spectral properties of vertebrate visual pigments. Vision Res. **34:** 1359–1369.

Hubbard, R., and A. Kropf, 1958 The action of light on rhodopsin. Proc. Natl. Acad. Sci. USA **44:** 130–139.

Huchon, D., F. M. Catzeflis and J. P. Douzery, 1999 Molecular evolution of the nuclear von Willebrand factor gene in mammals and the phylogeny of rodents. Mol. Biol. Evol. **16:** 577–589.

Jacobs, G. H., 1993 The distribution and nature of color vision among mammals. Biol. Rev. **68:** 413–471.

Johnson, R., K. B. Grant, T. C. Zankel, M. F. Boehn, S. L. Merbs *et al.*, 1993 Cloning and expression of goldfish opsin sequences. Biochemistry **32:** 208–214.

Jones, D. T., W. R. Taylor and J. M. Thornton, 1992 The rapid generation of mutation data matrices from protein sequences. Comput. Appl. Biosci. **8:** 275–282.

Kalmus, H., 1965 *Diagnosis and Genetics of Defective Colour Vision*. Pergamon Press, Oxford.

Kawamura, S., and S. Yokoyama, 1998 Functional characterization of visual and nonvisual pigments of American chameleon (*Anolis carolinensis*). Vision Res. **38:** 37–44.

Kawamura, S., N. S. Blow and S. Yokoyama, 1999 Genetic analyses of visual pigments of the pigeon (*Columba livia*). Genetics **153:** 1839–1850.

Khorana, H. G., B. E. Knox, F. Nasi, R. Swanson and D. A. Thompson, 1988 Expression of a bovine rhodopsin gene in *Xenopus* oocytes: demonstration of light-dependent ionic currents. Proc. Natl. Acad. Sci. USA **85:** 7917–7921.

Kleinschmidt, J., and F. I. Harosi, 1992 Anion sensitivity and spectral tuning of cone visual pigments in situ. Proc. Natl. Acad. Sci. USA **89:** 9181–9185.

Kumar, S., and S. B. Hedges, 1998 A molecular timescale for vertebrate evolution. Nature **392:** 917–920.

Liu, F.-G. R., and M. M. Miyamoto, 1999 Phylogenetic assessment of molecular and morphological data for Eutherian mammals. Syst. Biol. **48:** 54–64.

Madsen, O., M. Scally, C. J. Douady, D. J. Kao, R. W. Debry *et al.*, 2001 Parallel adaptive radiations in two major clades of placental mammals. Nature **409:** 610–614.

Merbs, S. L., and J. Nathans, 1992 Absorption spectrum of human cone pigments. Nature **356:** 433–435.

Merbs, S. L., and J. Nathans, 1993 Role of hydroxyl-bearing amino acids in differentially tuning the absorption spectra of the human red and green cone pigments. Photochem. Photobiol. **58:** 706–710.

Murphy, W. J., E. Eizirik, W. E. Johnson, Y. P. Zhang, O. A. Ryder *et al.*, 2001 Molecular phylogenetics and the origin of placental mammals. Nature **409:** 614–618.

Nathans, J., D. Thomas and D. S. Hogness, 1986 Molecular genetics of human color vision: the genes encoding blue, green, and red pigments. Science **232:** 193–201.

Nei, M., J. Zhang and S. Yokoyama, 1997 Color vision of ancestral organisms of higher primates. Mol. Biol. Evol. **14:** 611–618.

Neitz, M., J. Neitz and G. H. Jacobs, 1991 Spectral tuning of pigments underlying red-green color vision. Science **252:** 971–974.

Novacek, M. J., 1992 Mammalian phylogeny: shaking the tree. Nature **356:** 121–125.

Okano, T., Y. Fukada, I. G. Artamonov and T. Yoshizawa, 1989 Purification of cone visual pigments from chicken retina. Biochemistry **28:** 8848–8856.

Oprian, D. D., A. B. Asenjo, N. Lee and S. L. Pelletier, 1991 Design, chemical synthesis, and expression of genes for the three human color vision pigments. Biochemistry **30:** 11367–11372.

Palacios, A. G., F. J. Varela, R. Srivastava and T. J. Goldsmith, 1998 Spectral sensitivity of cones in the goldfish, *Carassius auratus*. Vision Res. **38:** 2135–2146.

Palczewski, K., T. Kumasaka, T. Hori, C. A. Behnke, H. Motoshima *et al.*, 2000 Crystal structure of rhodopsin: a G protein-coupled receptor. Science **289:** 739–745.

Radlwimmer, F. B., and S. Yokoyama, 1997 Cloning and expression of the red visual pigment gene of goat (*Capra hircus*). Gene **198:** 211–215.

Radlwimmer, F. B., and S. Yokoyama, 1998 Genetic analyses of the green visual pigments of rabbit (*Oryctolagus cuniculus*) and rat (*Rattus norvegicus*). Gene **218:** 103–109.

Searle, S. R., 1971 *Linear Models*. John Wiley & Sons, New York.

Shoshani, J., and M. C. McKenna, 1998 Higher taxonomic relationships among extant mammals based on morphology, with selected comparisons of results from molecular data. Mol. Phylogenet. Evol. **9:** 572–584.

Smith, W. C., and T. H. Goldsmith, 1990 Phylogenetic aspects of the distribution of 3-hydroretinal in the class Insecta. J. Mol. Evol. **30:** 72–84.

Sun, H., J. P. Macke and J. Nathans, 1997 Mechanisms of spectral tuning in the mouse green cone pigment. Proc. Natl. Acad. Sci. USA **94:** 8860–8865.

Thompson, I., 1991 Considering the evolution of vertebrate neural retina, pp. 136–151 in *Evolution of the Eye and Visual Systems*, edited by T. R. Cronly-Dillon and R. L. Gregory. CRC Press, Boca Raton, FL.

Waddell, P. J., Y. Cao, J. Hauf and M. Hasegawa, 1999a Using novel phylogenetic methods to evaluate mammalian mtDNA, including amino acid-invariant sites-LogDet plus site stripping, to detect internal conflicts in the data, with special reference to the position of hedgehog, armadillo, and elephant. Syst. Biol. **48:** 31–53.

Waddell, P. J., Y. Cao, M. Hasegawa and D. P. Mindell, 1999b Assessing the Cretaceous superordinal divergence times within birds and placental mammals by using whole mitochondrial protein sequences and an extended statistical framework. Syst. Biol. **48:** 119–137.

Walls, G. I., 1942 *The Vertebrate Eye and Its Adaptive Radiation*. The Cranbook Institute of Science, Bloomfield Hills, MO.

Whitmore, A. V., and J. K. Bowmaker, 1989 Seasonal variation in cone sensitivity and short-wave absorbing visual pigments in the rudd *Scadinius erythrophthalmus*. J. Comp. Physiol. A **166:** 103–115.

Winderickx, J., D. T. Lindsey, E. Sanocki, D. Y. Teller, A. G. Motulsky *et al.*, 1992 Polymorphism in red photopigment underlies variation in color matching. Nature **356:** 431–433.

Witkovsky, P., J. S. Levine, G. A. Engbretson, G. Hassin and E. F. Macnicol, 1981 A microspectrophotometric study of normal and artificial rod in the Xenopus retina. Vision Res. **21:** 867–873.

Yang, Z., 1997 PAML: a program package for phylogenetic analysis by maximum likelihood. Comput. Appl. Biosci. **13:** 555–556.

Yang, Z., S. Kumar and M. Nei, 1995 A new method of inference

of ancestral nucleotide and amino acid sequences. Genetics **141:** 1641–1650.

Yokoyama, R., and S. Yokoyama, 1990 Convergent evolution of the red- and green-like visual pigment genes in fish, *Astyanax fasciatus*, and human. Proc. Natl. Acad. Sci. USA **87:** 9315–9318.

Yokoyama, R., B. E. Knox and S. Yokoyama, 1995 Rhodopsin from the fish, Astyanax: role of tyrosine 261 in the red shift. Invest. Ophthalmol. Visual Sci. **36:** 939–945.

Yokoyama, S., 1997 Molecular genetic basis of adaptive selection: examples from color vision in vertebrates. Annu. Rev. Genet. **31:** 311–332.

Yokoyama, S., 1999 Molecular bases of color vision in vertebrates. Genes Genet. Syst. **74:** 189–199.

Yokoyama, S., 2000a Molecular evolution of vertebrate visual pigments. Prog. Retin. Eye Res. **19:** 385–419.

Yokoyama, S., 2000b Phylogenetic analysis and experimental approaches to study color vision in vertebrates. Methods Enzymol. **315:** 312–325.

Yokoyama, S., and N. S. Blow, 2001 Molecular evolution of the cone visual pigments in the pure rod-retina of the nocturnal gecko, *Gekko gekko*. Gene (in press).

Yokoyama, S., and F. B. Radlwimmer, 1998 The "five-sites" rule and the evolution of red and green color vision in mammals. Mol. Biol. Evol. **15:** 560–567.

Yokoyama, S., and F. B. Radlwimmer, 1999 The molecular genetics and evolution of red and green color vision in mammals. Genetics **153:** 919–932.

Yokoyama, S., and R. Yokoyama, 1989 Molecular evolution of human visual pigment genes. Mol. Biol. Evol. **6:** 186–197.

Yokoyama, S., and R. Yokoyama, 1996 Adaptive evolution of photoreceptors and visual pigments in vertebrates. Annu. Rev. Ecol. Syst. **27:** 543–567.

Yokoyama, S., N. S. Blow and F. B. Radlwimmer, 2000 Molecular evolution of color vision of zebra finch. Gene **259:** 17–24.

Communicating editor: S. W. Schaeffer

APPENDIX

Consider the relationships

$$
\begin{aligned}
Z + e_1 &= 560\\
\theta_{180} + Z + e_2 &= 553\\
\theta_{180} + \theta_{277} + \theta_{285} + \theta_{180\times285} + \theta_{277\times285} + \theta_{180\times277\times285} + Z + e_3 &= 530\\
Z + e_4 &= 561\\
\theta_{180} + Z + e_5 &= 553\\
\theta_{180} + \theta_{285} + \theta_{180\times285} + Z + e_6 &= 539\\
\theta_{180} + Z + e_7 &= 533\\
\theta_{180} + \theta_{277} + \theta_{285} + \theta_{180\times285} + \theta_{277\times285} + \theta_{180\times277\times285} + Z + e_8 &= 531\\
\theta_{180} + \theta_{308} + Z + e_9 &= 524\\
\theta_{180} + \theta_{277} + Z + e_{10} &= 545\\
\theta_{180} + Z + e_{11} &= 553\\
\theta_{180} + \theta_{197} + \theta_{308} + \theta_{180\times197} + \theta_{197\times308} + Z + e_{12} &= 509\\
\theta_{197} + \theta_{285} + Z + e_{13} &= 516\\
\theta_{197} + Z + e_{14} &= 532\\
\theta_{180} + \theta_{197} + \theta_{180\times197} + Z + e_{15} &= 534\\
\theta_{180} + \theta_{197} + \theta_{308} + \theta_{180\times197} + \theta_{197\times308} + Z + e_{16} &= 509\\
\theta_{180} + \theta_{197} + \theta_{308} + \theta_{180\times197} + \theta_{197\times308} + Z + e_{17} &= 508\\
Z + e_{18} &= 561\\
Z + e_{19} &= 559\\
Z + e_{20} &= 560\\
Z + e_{21} &= 560\\
\theta_{180} + \theta_{277} + \theta_{285} + \theta_{180\times285} + \theta_{277\times285} + \theta_{180\times277\times285} + Z + e_{22} &= 527\\
Z + e_{23} &= 557\\
Z + e_{24} &= 559\\
Z + e_{25} &= 558\\
\theta_{180} + \theta_{277} + \theta_{285} + \theta_{180\times285} + \theta_{277\times285} + \theta_{180\times277\times285} + Z + e_{26} &= 530,
\end{aligned}
$$

where e_i's ($i = 1, 2, \ldots, 26$) denote random errors.

This is represented in a matrix form as

$$\mathbf{y} = \mathbf{X} + \mathbf{e},$$

where

$$\mathbf{y}' = [560\ 530\ 561\ \ldots\ 530],$$

$$
\mathbf{X}' = \begin{bmatrix}
0&1&1&0&1&1&1&1&1&1&1&1&0&0&1&1&1&0&0&0&0&1&0&0&0&1\\
0&0&0&0&0&0&0&0&0&0&0&1&1&1&1&1&1&1&0&0&0&0&0&0&0&0\\
0&0&1&0&0&0&0&1&0&1&0&0&0&0&0&0&0&0&0&0&0&1&0&0&0&1\\
0&0&1&0&0&1&0&1&0&0&0&0&1&0&0&0&0&0&0&0&0&1&0&0&0&1\\
0&0&0&0&0&0&0&0&1&0&0&1&0&0&0&1&1&0&0&0&0&0&0&0&0&0\\
0&0&0&0&0&0&0&0&0&0&0&0&1&0&0&1&1&1&0&0&0&0&0&0&0&0\\
0&0&1&0&0&1&0&1&0&0&0&0&0&0&0&0&0&0&0&0&0&1&0&0&0&1\\
0&0&0&0&0&0&0&0&0&0&0&1&0&0&0&1&1&0&0&0&0&0&0&0&0&0\\
0&0&1&0&0&0&0&1&0&0&0&0&0&0&0&0&0&0&0&0&0&1&0&0&0&1\\
0&0&1&0&0&0&0&1&0&0&0&0&0&0&0&0&0&0&0&0&0&1&0&0&0&1\\
1&1&1&1&1&1&1&1&1&1&1&1&1&1&1&1&1&1&1&1&1&1&1&1&1&1
\end{bmatrix},
$$

and

$$\mathbf{e}' = [e_1\ e_2\ e_3\ \ldots\ e_{26}].$$

If we assume that the random term, **e**, has a normal distribution with mean **0** and $\sigma^2\mathbf{I}$, then the mean ($\hat{\theta}$) and standard error ($\hat{s}$) of $\boldsymbol{\theta}' = [\theta_{180}\ \theta_{197}\ \theta_{277}\ \theta_{285}\ \theta_{308}\ \theta_{180\times197}\ \theta_{180\times285}\ \theta_{197\times308}\ \theta_{277\times285}\ \theta_{180\times277\times285}\ Z]$ are estimated from

$$\hat{\theta} = (\mathbf{X}'\mathbf{X})^{-1}\mathbf{X}'\mathbf{y},$$

$$\hat{s} = [(\mathbf{X}'\mathbf{X})^{-1}\mathrm{SSE}/(n - p)]^{1/2},$$

where

$$\mathrm{SSE} = (\mathbf{y} - \mathbf{X}\hat{\theta})'(\mathbf{y} - \mathbf{X}\hat{\theta}),$$

and n and p denote the number of samples and parameters, respectively (Searle 1971).